КОРОТКИЕ СООБЩЕНИЯ

Optical elements based on silicon photonics

M.A. Butt [1], S.N. Khonina [1,2], N.L. Kazanskiy [1,2]
[1] Samara National Research University, 443086, Russia, Samara, Moskovskoye Shosse 34,
[2] IPSI RAS – Branch of the FSRC "Crystallography and Photonics" RAS,
Molodogvardeyskaya 151, 443001, Samara, Russia

Abstract

Silicon photonics is gaining substantial impulse because it permits optical devices to be realized inexpensively using standard semiconductor fabrication techniques and integrated with microelectronic chips. In this paper, we designed few optical elements such as optical power splitter, polarization beam splitter and Bragg grating based on silicon platform simulated using finite element method.

Keywords: optical power splitter, polarization beam splitter, Bragg grating, finite element method.

Citation: Butt MA, Khonina SN, Kazanskiy NL. Optical elements based on silicon photonics. Computer Optics 2019; 43(6): 1079-1083. DOI: 10.18287/2412-6179-2019-43-6-1079-1083.

Acknowledgements: This work was financially supported by the Russian Foundation for Basic Research (grant No. 18-29-20045_mk) for numerical calculations, by the Ministry of Science and Higher Education within the State assignment FSRC "Crystallography and Photonics" RAS (No. 007-GZ/Ch3363/26) for theoretical results.

Introduction

Moore's law in 1965 proposed that the number of transistors on an integrated circuit would double every two years has become an inspiration that continues to drive the electronics industry [1]. In 1965, integrated circuits comprised of 30-transistor devices have grown exponentially to today's high-end microprocessors beyond 500 million transistors integrated on a silicon chip the size of a fingernail. Silicon is considered as the best possible material for electronics and has been used in several photonic devices. The processing of silicon has been developed by the electronics industry to a level that is more than adequate for most integrated optical applications. Silicon, in fact, has various properties conductive to fiber optics. The band gap of silicon (~1.1 eV) is such that the material is transparent to infrared wavelength range usually used for optical transport [2]. Alike optical fiber, these optical waveguides (WG) can be used to confine and steer light as it passes through the silicon WG core. Due to the wavelengths typically used for optical transport and silicon's high index of refraction, the feature sizes required for processing these silicon WGs are on the order of 0.3–1 μm. The lithography requirements needed to process WGs with these sizes are easily available today [3].

Additionally, the same carriers used for the basic functionality of the transistor can be used to modulate the phase of light passing through silicon WGs and thus create "active" photonic devices. If all this remains CMOS-compatible, it could be possible to process transistors alongside photonic devices, the combination of which could bring new levels of performance, functionality, power and size reduction, all at a lower cost. That is why integrated optics in silicon is interesting for a combination of technological and cost reasons.

Based on remarkably advance silicon semiconductor technology, silicon photonics would deliver with a low-cost, highly integrated electronic-photonic platform, in which ultra-compact photonic devices and electronic circuits are united. The ultimate motive behind silicon photonics is the ability to use CMOS-like fabrication resulting in high volume production at low cost [4]. In this paper, we designed optical power splitter, Bragg gratings and polarization beam splitter based on a silicon platform. All the simulations are performed by using Comsol Multiphysics 5.1 which solves the Helmholtz equation with the finite element method (FEM).

Optical power splitter

Optical power splitters (OPS) play a significant role in optical communication systems [5] and periodic optical sources for integrated microfluidic devices. OPSs are mainly based on either Y-branch splitters [6, 7] or multimode interference (MMI) splitters [8]. In this paper, we modelled 1×4 OPS 8 μm long based on coupled- mode theory (CMT) [9] by using seven vertically slotted WGs at 1550 nm TE-polarized light. In our previous work, we proposed 1×8 T-shape balanced optical power splitter based on 90º bend asymmetric vertical slot WGs [10]. A slot WG has a unique structure that strengthens the light inside a nanometer-scale region of low index material (can be air) that is bounded by two layers of high index material [11, 12]. Strong light confinement in the slot is due to the discontinuity of the E-field perpendicular to the interface between materials with low and high refractive indices.

Numerical optimizations are carried out on the coupling gap (C1, C2 and C3) between the slot WGs structures (by keeping the coupling lengths constant) in order to attain an identical power distribution among 4 outputs. The CMT is used to evaluate the mode coupling or con-

version in optical WGs. The physical models for coupled WG systems contain two or more dielectric WGs placed in close proximity. These WGs may be parallel to each other or may have variable separations. The splitter schematic structure is shown in fig 1. And the slot WG cross-section is described by the inset. The coupling strength is very sensitive to the distance between the WGs and it is essential to eventually select a design that can function effectively given the type of deficiencies that are probable from the manufacturing process.

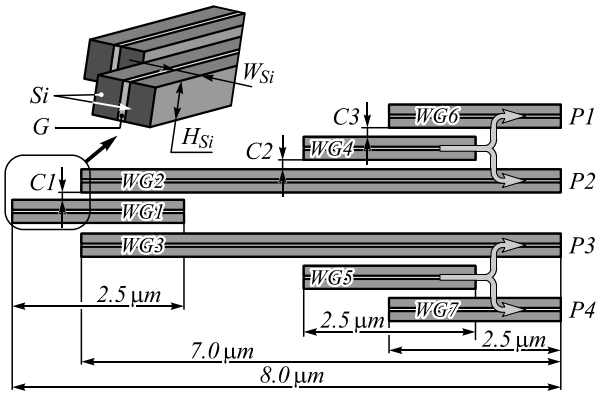

Fig. 1. Schematic of a 1×4 OPS based on seven vertical slot WGs

In the first stage, C1 is varied from 30–200 nm between WG1 and the adjacent WGs (2 and 3). The coupling efficiency of C1 is plotted in fig. 2*a*). It can be observed that when C1 is too narrow, that is <45 nm, the energy doesn't transfer to the adjacent WGs instead it confines itself in C1. This is due to the fact that the gap is too small that it behaves as another slot WG and confine the E-field in C1.

A maximum coupling efficiency is obtained at values between 90–125 nm (fig. 2*a*) where the power is equally divided between WG2 and WG3 with less coupling losses. Hence, we used a finest value of C1 = 115 nm in our splitter design for maximum coupling. For simplification reason, C2 is fixed at 115 nm to obtain maximum coupling between WGs (2, 4) and WGs (3, 5). In order to obtain the balanced 1×4 OPS, *C3* has to be slightly adjusted. The distribution of the power between WG3 and WG7 is not equal as seen in fig. 2*b*) where normalized intensity distribution at port 1, port 2, port 3 and port 4 are shown for various values of C3. For values of C3 < 140 nm, the output intensity at Port 2 and Port 3 is less than Port 1 and Port 4. The optimized value of C3 is obtained at 140 nm where the OPS is balanced with 25 % of power transmission at each port as shown in fig. *2b*). The line graph at Port 1, Port 2, Port 3 and Port 4 is shown in fig. 2*c*.

Polarization beam splitter

A polarization beam splitter (PBS) is one of the most important components in modern optical communication systems and is used to separate the two orthogonal polarizations of light [13, 14]. The working principle of conventional PBS devices is based on either modal evolution or interferometry. Several devices such as multimode interference couplers, directional couplers (DCs) [15] and Mach–Zehnder interferometers are based on the principle of interferometry. Among these, PBS devices based on DCs are preferred because they are generally compact in size. In this paper, we propose a fairly simple and compact PBS design based on two silicon strip WGs separated by a Bridge WG as shown in fig. 3. $L1 = L2 = 12$ μm, which is the length of WG1 and WG2. Light with either polarization TE/TM is coupled at WG1 (input WG). TE-polarized light is collected from WG1 whereas TM-polarized light is coupled through a Bridge WG and collected at WG2.

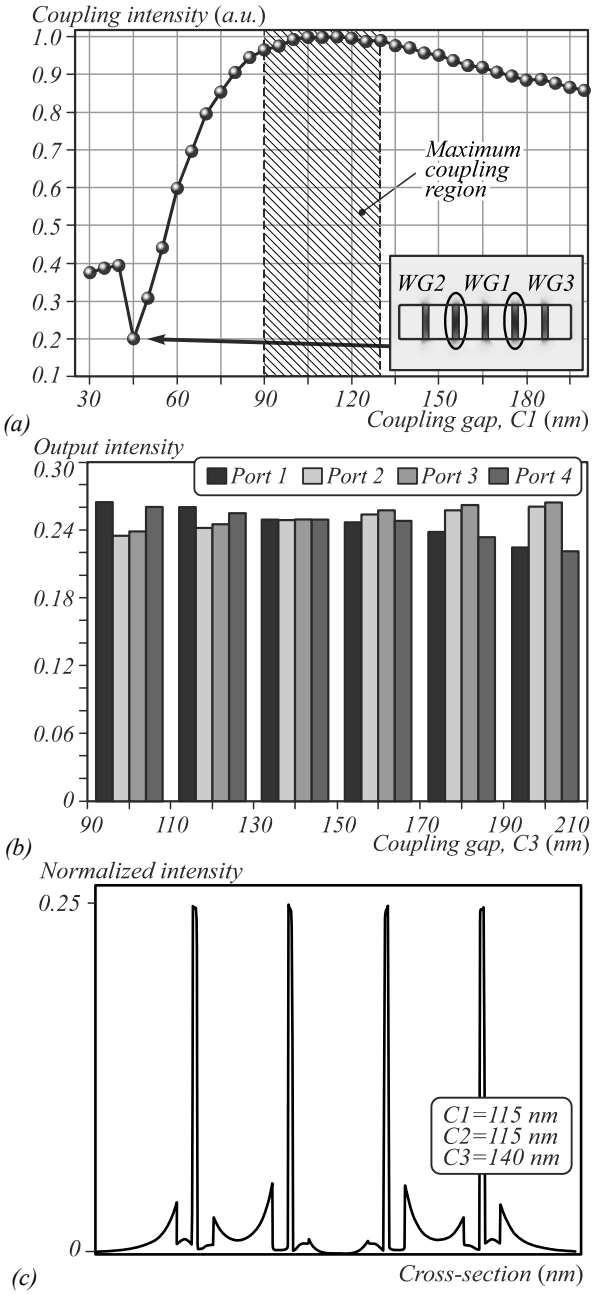

Fig. 2. (a) Coupling efficiency vs coupling gap (C1), (b) coupling gap (C3) versus intensity distribution at Port 1, Port 2, Port 3 and Port 4, (c) normalized intensity at Port 1, Port 2, Port 3 and Port 4

Si WGs have large polarization mode dispersion (PMD) [16] owing to their structural birefringence. That is why there is a significant difference in the coupling lengths between the two polarization modes due to the

different propagation constant initiated by the PMD. When a TM-polarized light is coupled into WG1, the light beam is transferred to WG2 after propagating through a coupling length. As a substitute, the TE-polarized light usually has a longer coupling length than the TM-polarized light does, therefore the TE-polarized light travels in the same WG, without coupling to the other WG, after propagating through the same coupling length. In our design, the coupling efficiency of the TM-mode intensely depends on the length of the bridge WG (LBWG). We present the contour plot of the TM-mode at the output of the PBS (fig. 4*a*–*d*).

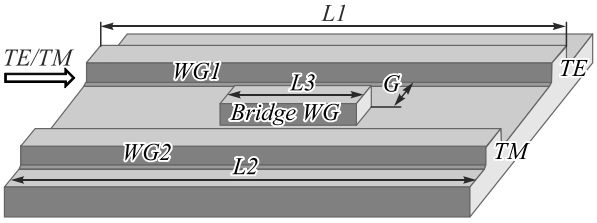

Fig. 3. Schematic of a PBS

Si WGs have large polarization mode dispersion (PMD) [16] owing to their structural birefringence. That is why there is a significant difference in the coupling lengths between the two polarization modes due to the different propagation constant initiated by the PMD. When a TM-polarized light is coupled into WG1, the light beam is transferred to WG2 after propagating through a coupling length. As a substitute, the TE-polarized light usually has a longer coupling length than the TM-polarized light does, therefore the TE-polarized light travels in the same WG, without coupling to the other WG, after propagating through the same coupling length. In our design, the coupling efficiency of the TM-mode intensely depends on the length of the bridge WG (LBWG). We present the contour plot of the TM-mode at the output of the PBS (fig. 4*a*–*d*).

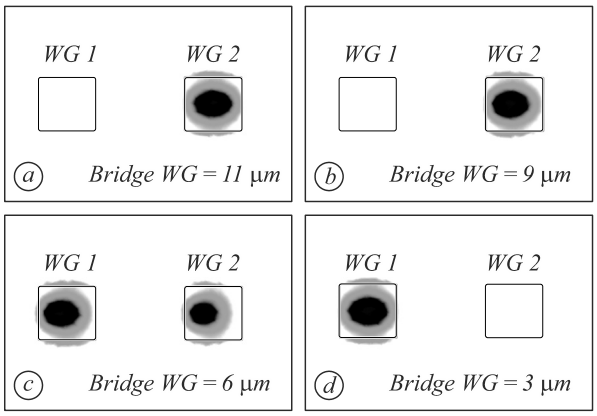

Fig. 4. Contour plot of TM mode at the output of PBS based on silicon strip WGs

The L_{BWG} varies from 2 to 11 μm with a step size of 1 μm. When $L_{BWG} \geq 9$ μm, the TM-mode has a maximum coupling efficiency, as shown in fig. 4*a* and 4*b*. At $L_{BWG} = 6$ μm, the design acts as a power divider for the TM polarization only as shown in fig. 4*c*; at $L_{BWG} = 3$ μm, no coupling of the TM-mode takes place as shown in fig. 4*d*. The amount of power coupled is decided by the overlap of the modes in the separate channels. Thus, it depends on the WG's separation (G) and the interaction length (L_{BWG}). The value of G between the WGs plays an important role in the coupling of the TM-mode from WG1 to WG2 while also maintaining the TE-mode in WG1. We keep the value of G identical between the WG1-Bridge WG and the Bridge WG-WG2. The mode power of TE and TM was calculated at 1550 nm in WG1 and WG2, respectively, for G varies between 50–150 nm. At $G < 50$ nm, the mode power of both TE/TM polarizations in the WGs is inconsiderable because the light is mostly confined to the G. The maximum value of the TE- and TM-modes was obtained at $G = 150$ and 120 nm, respectively. So there is a slight compromise in selecting the optimum value of G where both the modes can have high values. Hence, for our PBS design, we choose $G = 120$ nm where both polarizations have more than 70% mode power, as shown in fig. 5.

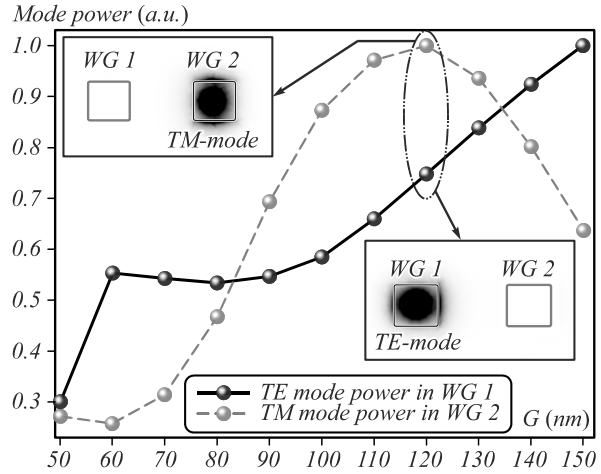

Fig. 5. Mode power vs coupling gap (G)

Bragg grating (BG)

Bragg gratings (BG) are optical elements with spatially, periodically varying refractive indices. They are not only used in telecommunication but also extensively used as temperature, strain, pressure, current and (bio) chemical sensors [17, 18]. Bragg gratings can be incorporated into planar WG structures at a high integration density. Bragg gratings back-reflect a certain wavelength within the WG instead of coupling it in or out such as grating couplers. We designed a Fabry–Perot resonator based on silicon slot WG. In slot WG, the guided light is strongly confined within a narrow low-index slot (S) between the two high indices photonic wires. There are two claddings (high index material). In our design, we are considering air ($n = 1$) as a slot and Si ($n = 3.45$) as a high index material. The electric field propagating in the slot go through interference at the high contrast interface which makes the electromagnetic wave to confine intensely in the narrow slot than in the cladding. This leads to the implementation of compact and high-performance photonic components such as resonators and polarization beam splitters. The width of a silicon slot WG are denoted as W. The height (H) of the WG structure is fixed at 0.22 μm.

The slot and depth of grating are represented by S and d, respectively as shown in fig. 6.

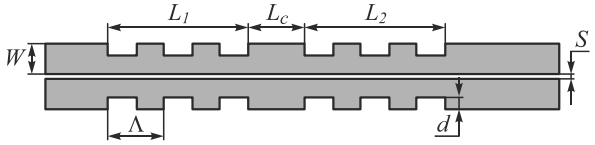

Fig. 6. Schematic of Bragg gratings and cavity on both sides of the silicon slot WG

The transmission spectrum of the FP-resonator based on slot WG is demonstrated for a number of the grating period (N_G) = 20 and 30 by maintaining the d = 30 nm as shown in figure 7. It is observed that the FWHM and FSR is about 3.1 nm and 43 nm, respectively for N_G = 20. Whereas, for N_G = 30, the FWHM and FSR is around 2.1 nm and 34 nm, respectively. This clearly shows that we can control the spectral characteristics by manipulating the number of grating periods.

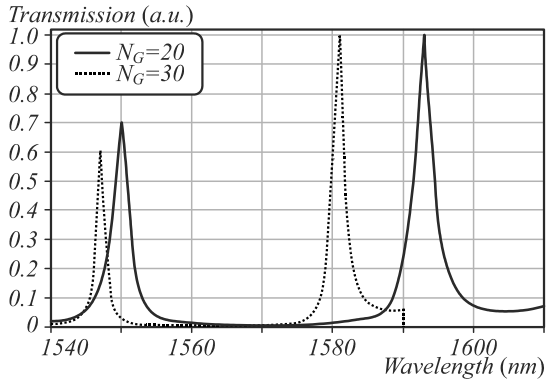

Fig. 7. Transmission spectrum of a FP-resonator for N_G=20 and 30, where H=0.22 μm, W=0.27 μm, S= 50 nm, L_c= 0.5 μm, d=30nm

The electric field distribution of *FP*-resonator for N_G = 30 is plotted in fig. 8. The varying transmission function of a *FP*-resonator is produced due to the interference between the multiple reflections of light between two DBRs. If the transmitted beams are out of phase then destructive interference takes place which corresponds to a minimum or zero transmission as shown in fig. 8*a*. Whereas if the transmitted beams are in phase therefore constructive inference takes place and this delivers a high transmission peak of the resonator as demonstrated in fig. 8*b*.

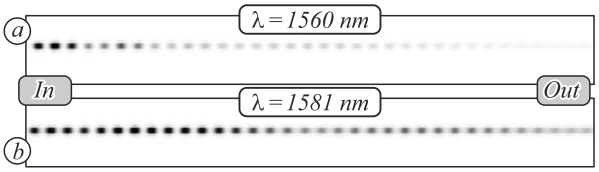

Fig. 8. The E-field distribution in the Bragg grating at, (a) H/2 for 1560 nm, (b) H/2 for 1581 nm

Conclusion

In this work, we proposed a compact design of 1×4 balanced optical power splitter, polarization beam splitter and Bragg grating based on a silicon platform. The design parameters are discussed in detail in order to obtain the best performance of the device. The design parameters are realistic and easy to fabricate with the available CMOS technology. We believe that this study will help the researchers from all over the world in order to develop new compact photonic devices based on a silicon platform.

References

[1] Wu J, Shen YL, Reinhardt K, Szu H, Dong B. A nanotechnology enhancement to Moore's law. Applied Computational Intelligence and Soft Computing 2012; 2013: 1-13. DOI: 10.1155/2013/426962.

[2] Xin XK. An indirect measurement of energy gap for silicon and germanium. Solid-State Electronics 1986; 29(9): 845-847. DOI: 10.1016/0038-1101(86)90001-8.

[3] Dong J, Liu J, Kang G, Xie J, Wang Y. Pushing the resolution of photolithography down to 15 nm by surface plasmon interference. Sci Rep 2014; 4: 5618. DOI: 10.1038/srep05618.

[4] Radamson HH, et al. Miniaturization of CMOS. Micromachines 2019; 10: 293. DOI: 10.3390/mi10050293.

[5] Huilian M, Jianyi Y, Xiaoqing J, Minghua W. Compact and economical MMI optical power splitter for optical communication. 2000 International Conference on Communication Technology Proceedings (Cat. No.00EX420) 200: 1561-1564. DOI: 10.1109/ICCT.2000.890959.

[6] Burtscher C, Seyringer D, Kuzma A, Lucki M. Modeling and optimization of 1x32 Y-branch splitter for optical transmission systems. Optical and Quantum Electronics 2017; 49: 396. DOI: 10.1007/s11082-017-1228-8.

[7] Butt MA, Kozlova ES, Khonina SN. Modeling of a straight channel and Y-splitter waveguides by loading SiO2 planar waveguide with MgF2. Progress in Electromagnetics Research Symposium – Spring (PIERS) 2017: 2472-2477. DOI: 10.1109/PIERS.2017.8262167.

[8] Malka D, Danan Y, Ramon Y, Zalevsky Z. A photonic 1x4 power splitter based on multimode interference in silicon-gallium-nitride slot waveguide structures. Materials 2016; 9(7): 516. DOI: 10.3390/ma9070516.

[9] Huang W-P. Coupled-mode theory for optical waveguides: an overview. J Opt Soc Am A 1994; 11(3): 963-983. DOI: 10.1364/JOSAA.11.000963.

[10] Butt MA, Khonina SN, Kazanskiy NL. A T-shaped 1x8 balanced optical power splitter based on 90° bend asymmetric vertical slot waveguides. Laser Phys 2019; 29(4): 046207. DOI: 10.1088/1555-6611/ab0372.

[11] Butt MA, Khonina SN, Kazanskiy NL. Silicon on silicon dioxide slot waveguide evanescent field gas absorption sensor. J Mod Opt 2018; 65(2): 174-178. DOI: 10.1080/09500340.2017.1382596.

[12] Degtyarev SA, Butt MA, Khonina SN, Skidanov RV. Modelling of TiO2 based slot waveguides with high optical confinement in sharp bends. International Conference on Computing, Electronic and Electrical Engineering (ICE Cube) 2016: 10-13. DOI: 10.1109/ICECUBE.2016.7495222.

[13] Butt MA, Khonina SN, Kazanskiy NL. Compact design of a polarization beam splitter based on silicon-on-insulator platform. Laser Phys 2018; 28(11): 116202. DOI: 10.1088/1555-6611/aadf18.

[14] Huang J, Yang J, Chen D, He X, Han Y, Zhang J, Zhang Z. Ultra-compact broadband polarization beam splitter with strong expansibility. Photonics Research 2018; 6(6): 574-578. DOI: 10.1364/PRJ.6.000574.

[15] Chang LM, Liu L, Gong YH, Tan MQ, Yu YD, Li ZY. Polarization-independent directional coupler and polarization beam splitter based on asymmetric cross-slot waveguides. Appl Opt 2018; 57(4): 678-683. DOI: 10.1364/AO.57.000678.

[16] Rashleigh SC, Ulrich R. Polarization mode dispersion in single-mode fibers. Opt Lett 1978; 3(2): 60-62. DOI: 10.1364/OL.3.000060.
[17] Suresh R, Tjin SC, Hao J. Applications of fiber bragg grating sensors. In Book: Soh C-K, Yang Y, Bhalla S. Smart materials in structural health monitoring, control and biomechanics. Heidelberg, New York, Dordrecht, London: Springer; 2012. DOI: 10.1007/978-3-642-24463-6_12.
[18] Butt MA, Khonina SN, Kazanskiy NL. Numerical analysis of a miniaturized design of a Fabry–Perot resonator based on silicon strip and slot waveguides for bio-sensing applications. J Mod Opt 2019; 66(11): 1172-1178. DOI: 10.1080/09500340.2019.1609613.

Authors' information

Muhammad Ali Butt (b. 1985) received a Bachelor's degree in Electrical (Telecommunication) Engineering from Comsats Institute of Information and Technology, Pakistan in year 2008. He acquired his Master´s degree in Electrical Communication Engineering from University of Kassel, Germany (2010). He accomplished his PhD degree with Cum Laude in Material Sciences from Universitat Rovira i Virgili, Spain in year 2015. In 2013, he made a research stay at Optoelectronic research Centre (ORC), University of Southampton, England. Currently he works as a Senior Scientist at Samara National Research University, Russia. Research interests are optical waveguides, plasmonic sensors, diffractive optics, and optical filters. E-mail: *m.a.butt@ssau.ru* .

Svetlana Nikolaevna Khonina, Doctor of Physical and Mathematical Sciences; Professor of Samara National Research University. Main researcher of the IPSI RAS – Branch of the FSRC "Crystallography and Photonics" RAS. Research interests: diffractive optics, singular optics, mode and polarization transformations, optical manipulating, optical and digital image processing. E-mail: *khonina@ipsiras.ru* .

The information about author **Nikolay Lvovich Kazanskiy** you can find on page 955 of this issue.

Code of State Categories Scientific and Technical Information (in Russian – GRNTI)): 29.31.15, 29.33.43, 20.53.23.
Received July 03, 2019. The final version – September 05, 2019.